A Novel Electrode Architecture for Monitoring Rifampicin in Various Pharmaceuticals

Rajasekhar Chokkareddy, Natesh Kumar Bhajanthri[*] , Gan G Redhi[*]

Electroanalytical Laboratories, Department of Chemistry, Durban University of Technology, P.O Box 1334, Durban 4000, South Africa.
[*]E-mail: redhigg@dut.ac.za, nateshkumar786@gmail.com

The present work involves the fabrication of glassy carbon electrode (GCE) with iron oxide nanoparticles (Fe_3O_4NPs) and multiwalled carbon nanotubes (MWCNTs) composite. Further it was immobilized with Coenzyme q (Co en-q/ Fe_3O_4NPs/MWCNTs/GCE) to enhance the electrochemical performance of the modified electrode for the determination of rifampicin (RIF). The designed sensor was successfully characterized by Fourier transform infrared spectroscopy (FT-IR), transmission electron microscopy (TEM), thermo gravimetry (TGA) and x-ray diffraction (XRD) studies. The electrochemical oxidation of RIF has been studied by cyclic voltammetry (CV) and differential pulse voltammetric techniques (DPV). The enzyme immobilized sensor surface area was calculated and found to be 10.03 mm^2. This larger surface area was responsible for the oxidation of more number of RIF molecules on the surface of sensor. The RIF shows two anodic peaks at + 0.10 V and + 0.72 V in phosphate buffer solution (PBS) pH 7.5. The cyclic voltammetric measurements reveals that the developed sensor exhibited an enhanced electrochemical platform with an approximately eight-fold increment in the anodic peak currents. Under the optimized conditions, a good linear relationship was observed between peak currents and RIF concentration. The studied linearity range (2 – 20 μM) showed a limit of detection (LOD) of 0.032 μM, 0.413 μM and limit of quantification (LOQ) of 1.069 μM, 1.258 μM for anodic peaks I and peaks II respectively. The proposed sensor showed longstanding stability and high reproducibility. The method was successfully applied for the determination of RIF in pharmaceutical tablets without any sample pre-treatment.

1. INTRODUCTION

Infectious diseases are fatal enemies of the global population. Tuberculosis (TB) is an infection disease caused by *Mycobacterium tuberculosis*. However, TB is found in every country of the world, and in 2012, the largest number of new cases was reported in Asia and African countries, accounting for 80% of new cases globally. In order to prevent TB, rifampicin (3-[(4-methyl-1-piperazinyl) imino]

methyl rifamycin) has been prescribed as a single combination with first line anti TB drugs (isoniazid, pyrazinamide and ethambutol) at fixed dosages [1, 2]. The over dosage of RIF produces many side effects such as headaches, kidney damages, nausea, vomiting and liver diseases [3]. A literature survey reveals that several analytical methods, such as high-performance liquid chromatography [4-6], UV-Visible spectro photometric method [7], capillary electrophoresis [8], fluorimetry [9] and electroanalytical methods have been employed for the determination of RIF. However, most of the methods are expensive, complicated, require sample pretreatment, and expert knowledge of electrochemical methods. In electrochemical methods, cyclic voltammetry, differential pulse voltammetric techniques were majorly used in RIF analysis. The electrochemical method involving modified electrodes are receiving more attentions from researchers for the analysis of pharmaceutical samples. According to the literature survey, DNA-modified carbon paste electrodes [10], cyclodextrin based sensors [11], cytochrome P450-2E1 metabolised nano biosensors [12], HRP-based biosensors [13] have been reported for RIF analysis. However, the above mentioned electrode fabrication and the methodologies involves complexity and need highly sophisticated laboratory equipment and condition.

Currently, MWCNTs are widely used as an electrode coating material, due to the favourable specialized properties. It possess large specific surface area, good adsorption properties, electrochemical bond expansion, catalytic activities as well as good chemical and thermal stability [14]. They can be modified and functionalized there by making it suitable for anchoring the nanoparticles on the external surface and improving the sensitivity of the electrochemical response [15]. Metal oxide nanoparticles have numerous advantages such as high electron conductivity, biodegradability, low cost and simple preparation methods. Owing to these advantages of metal oxide nano particles, they are extensively used as anchoring electrochemical substances in modified sensors. In recent years, many metal oxide nanoparticles (CuO_2, TiO_2, Fe_3O_4, ZnO, and Ag_2O) have been used in biosensors for the fabrication of electrodes. Among these Fe_3O_4 nanoparticles has unique properties such as smaller particle size with larger surface area, provide enhanced selectivity and sensitivity for this method, and facilitate the electron transfer process at the electrode and without interference [16, 17]. Fe_3O_4 generally conjugates with enzymes it considers as biologically and electro catalytically active [18]. The Co en-q is a fat-soluble vitamin and functions as an antioxidant. Its performs as an electron transporter in the electron transport chain [19]. This facilitates the fast transfer of electrons from RIF to the electrode surface and leads to the enrichment of electroactivity of the fabricated sensor. Additionally, it generates the electrophilic site which increase the sensitivity and limits of detection of the fabricated electrode. In the present work GCE was coated with MWCNTs, it was further capped with Fe_3O_4NPs and finally immobilized with Co en-q for the determination of RIF. The aim of this work is to explore the potentialities of the biosensor and develop a novel, rapid and accurate voltammetric method for the determination of RIF in various pharmaceutical formulations. A voltammetric sensor was optimized by testing with many methods of electrode coating, and the best results were the use of Co en-q/ Fe_3O_4NPs/MWCNTs/GCE.

2. EXPERIMENTAL

2.1. Materials

Multiwalled carbon nanotubes (O.D. × 6-9 nm, 95% Carbon) and pure analytical grade of Rifampicin and Coenzyme-Q (≥95%) were purchased from Sigma Aldrich. N, N-dimethylformamide, sodium hydroxide, disodium hydrogen phosphate, sodium dihydrogen orthophosphate, sulfuric acid, ethanol, potassium bromide, iron (II) sulphate, nickel nitrate, acetic acid, folic acid, uric acid and iron (II) chloride tetrahydrate, were purchased from Capital Lab Suppliers (Durban, South Africa).

2.2. Instrumentation

Voltammetric measurements were performed with a 797VA Computrace from Metrohm (Herisau, Switzerland) equipped with the computrace 1.31 software. A glassy carbon electrode (3.0 mm diameter) or modified Co en-q/ Fe_3O_4NPs/MWCNTs/GCE as a working electrode, Ag/AgCl (saturated with KCl) reference electrode and platinum wire counter electrode were used for the electrochemical study. A digital pH meter (CRISON model 2000) was used for preparing the buffer solutions. The FT-IR spectra were recorded on Varian 800 FTIR Scimitar series spectrometer. Transmission electron microscope (TEM) images were obtained on a JEM 2100 LaB6 field emission transmission electron microscope. The TGA was performed with TGA/DSC1SF/1346 model, supplied with STAR^e software version 9.20 (Mettler Toledo). The entire experiment was carried out at room temperature. The working stock, standard and supporting electrolytic solutions were kept in the refrigerator at 4 ^{o}C.

2.3. Reagents

According to previous literature [20] with slight modification, 1.21 g (0.03 M) of $FeCl_2.4H_2O$ was dissolved in a 250 ml volumetric flask with deionized water. The 4 g (1 M) NaOH was dissolved in another 100 ml volumetric flask with deionized water. Further, 150 ml of $FeCl_2.4H_2O$ was taken into the 500 ml beaker and then slowly added 50 ml of 1M NaOH and subjected to heating at 100 ^{o}C on a hot plate for about 30 min with continuous stirring. After the completion of the reaction the reaction mixture turns into black colour precipitate from the original wine red colour. The precipitate was then washed several times with deionized water and filtered with Whatman-1 filter paper and then dried at 50 ^{o}C for 2 h. The newly formed Fe_3O_4NPs was kept in refrigerator for further use.

2.4. Preparation of Co en-q/ Fe_3O_4NPs/MWCNTs/GCE

Prior to use, the GCE was polished with an alumina slurry to obtain a mirror like surface, there after washed with deionized water and sonicated with ethanol and deionized water (50:50) to remove the alumina particles on electrode surface. It was finally rinsed with deionized water and dried in an oven. 0.10 mg of MWCNTs was dissolved in 4 ml of N, N-dimethyl formamide (DMF) and then kept

for ultra-sonication for 30 min, finally resulting in a black suspension, which was used for the modification of GCE.

Afterwards, 0.20 mg Fe_3O_4 and 0.20 mg of MWCNTs was dispersed into 5 ml of N, N-dimethyl formamide (DMF) by ultra-sonication for 1 h to give a black suspension. The resulting dispersion (5 μL Fe_3O_4/MWCNTs) was dropped on the surface of GCE and kept for drying in an oven at 50 $^\circ$C for about 10 min. The electrode was then cooled to room temperature and thereafter 2 μL of Co en-q enzyme was added, and coated electrode left undisturbed at 4 $^\circ$C for about 15 min for the complete enzyme immobilization process to occur, finally resulting in the Co en-q/ Fe_3O_4NPs/MWCNTs/GCE.

2.5. Preparation of tablet samples

Tablet samples containing RIF were purchased from the local pharmacy (Ebsar-2 Ds, R-Cin 600). The fabricated sensor was tested to determine the RIF in commercialized tablets via following procedure. Approximately 5-10 tablets were weighed and ground as a finely powdered sample. A 50 mg tablet sample was transferred into a 100 ml volumetric flask and dissolved in PBS. The resulting mixture was sonicated for 40 min. The analyses were performed via the standard addition method in DPV technique.

3. RESULTS AND DISCUSSION

3.1. Co en-q/ Fe_3O_4NPs/MWCNTs/GCE characterization
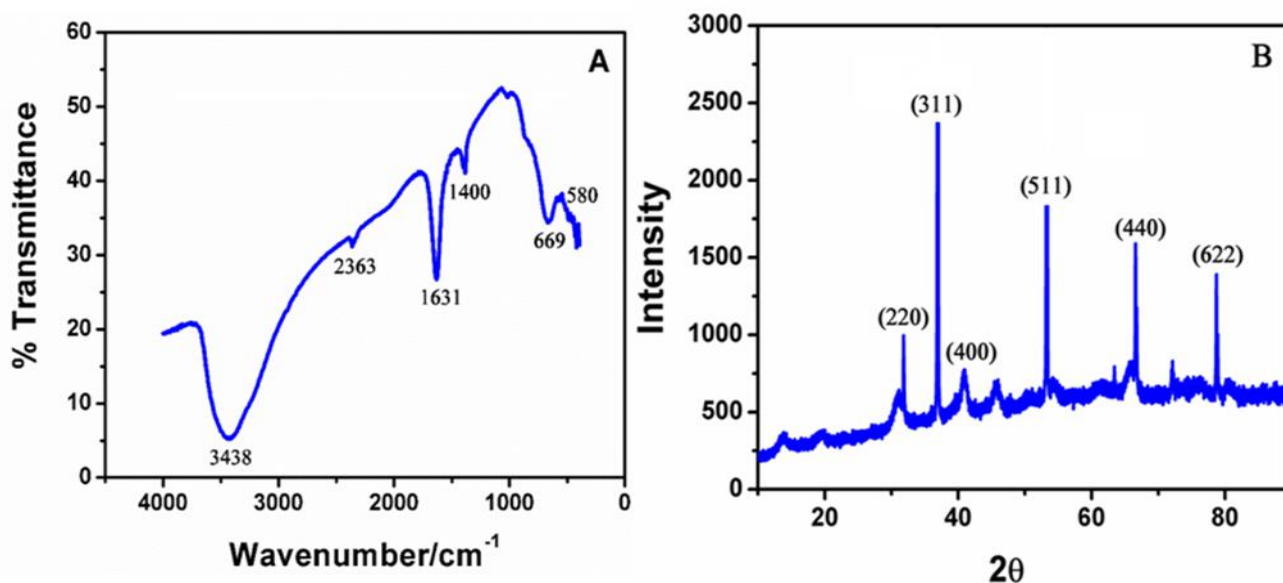
Figure 1. (**A**) FT-IR characterization of Fe_3O_4NPs. (**B**) XRD Image of Fe_3O_4NPs.

The FTIR spectra of the Fe_3O_4NPs are showed in fig. 1A. From the FTIR spectrum the band appeared at 580 cm^{-1} the peak associated with Fe-O presenting the tetrahedral side which can be attributed to Fe_3O_4 [21].The Fe_3O_4NPS can be seen by strong absorption band at around 669 cm^{-1} which corresponds to the Fe-O absorption. The band at 1400 cm^{-1} indicates –C-H bending vibrations.
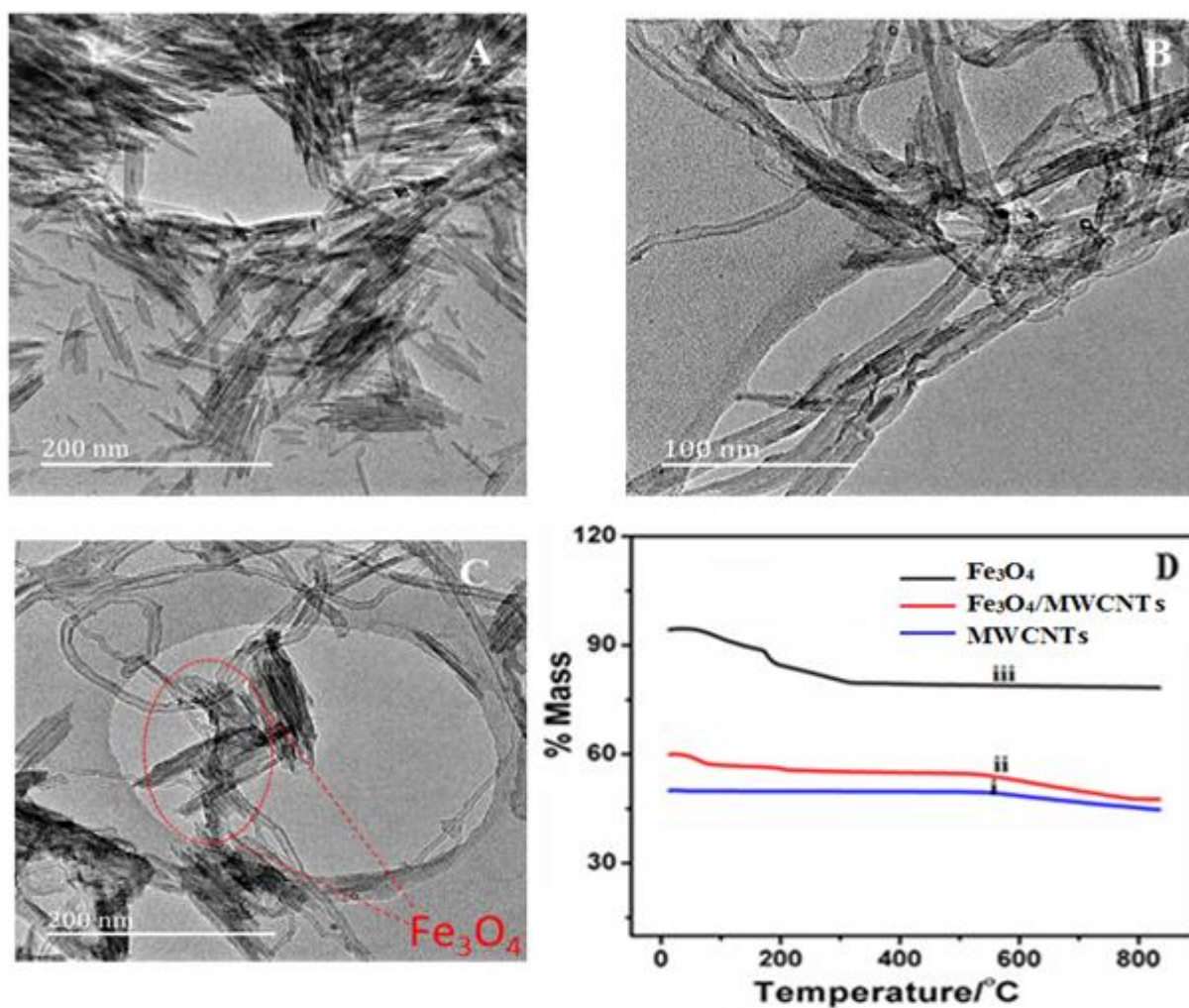
Figure 2. **(A)** TEM image Fe_3O_4NPs **(B)** Pure MWCNTs **(C)** MWCNTs- Fe_3O_4NPs **(D)** TGA curves for **(i)** MWCNTs **(ii)** Fe_3O_4NPs /MWCNTs and **(iii)** Fe_3O_4NPs

The intense band at 1631 cm^{-1} is attributed to stretching of OH mode of H_2O [22]. On the other hand the peak at 2363 cm^{-1} showed strong stretching of O=C=O. The peak at 3438 cm^{-1} is attributed to the stretching vibrations of OH arising from hydroxyl groups from the water on Fe_3O_4NPs [23]. Fig. 1B shown the x-ray diffraction pattern of the Fe_3O_4NPs. The Fe_3O_4NPs showed six specific peaks at 30.03^o, 35.52^o, 43.02^o, 53.6^o, 68.25^o and 76.32^o, corresponding to (220), (311), (400), (511), (440) and (622) respectively. The above strong diffraction intensities of the Fe_3O_4NPs reveals a the cubic spinal structure [24]. Fe_3O_4NPs shows a very high intensive peak at 35.52^o (311) indicating that the nanoparticles are ultrafine in nature, single cubic phase and small crystallite size. Based on the Debye-Scherer formula [25], the size of the Fe_3O_4NPs was also calculated and found to be approximately 15 nm in diameter.

$$d_{hkl} = \frac{0.9\,\lambda}{\beta\,Cos\,\theta} \tag{1}$$

Where β is the full width at half maximum value of XRD diffraction lines, λ is the wave length and θ is the half diffraction angle of 2θ.

Fig. 2A indicates TEM image of the synthesized Fe_3O_4NPS. These nanoparticles are in rod like geometry and they are aggregated like a bunch.

The fig. 2B clearly shown the tubular network like structure of MWCNTs. The fig. 2C shown reveals the adherence of Fe_3O_4NPS on the surface of the MWCNTs. Furthermore, the thermo gravimetric analysis of the MWCNTs, Fe_3O_4NPs/MWCNTs and Fe_3O_4NPs are shown in fig 2D. The thermograms for pure MWCNTs are shown with definite mass losses at 570 °C due to the carbon oxidation (black line fig. 2D). The Fe_3O_4NPs/MWCNTs shows that the mass losses at below 300 °C due to the loss of residual water in the sample [26]. On the other hand, the Fe_3O_4NPs losses minor mass at below 300 °C due to the evaporation of water. At 600 to 800 °C there is no significant mass loss, and this implies that there is only iron oxide at this range of temperature [27].

3.2. Electrochemical behavior of fabricated electrodes
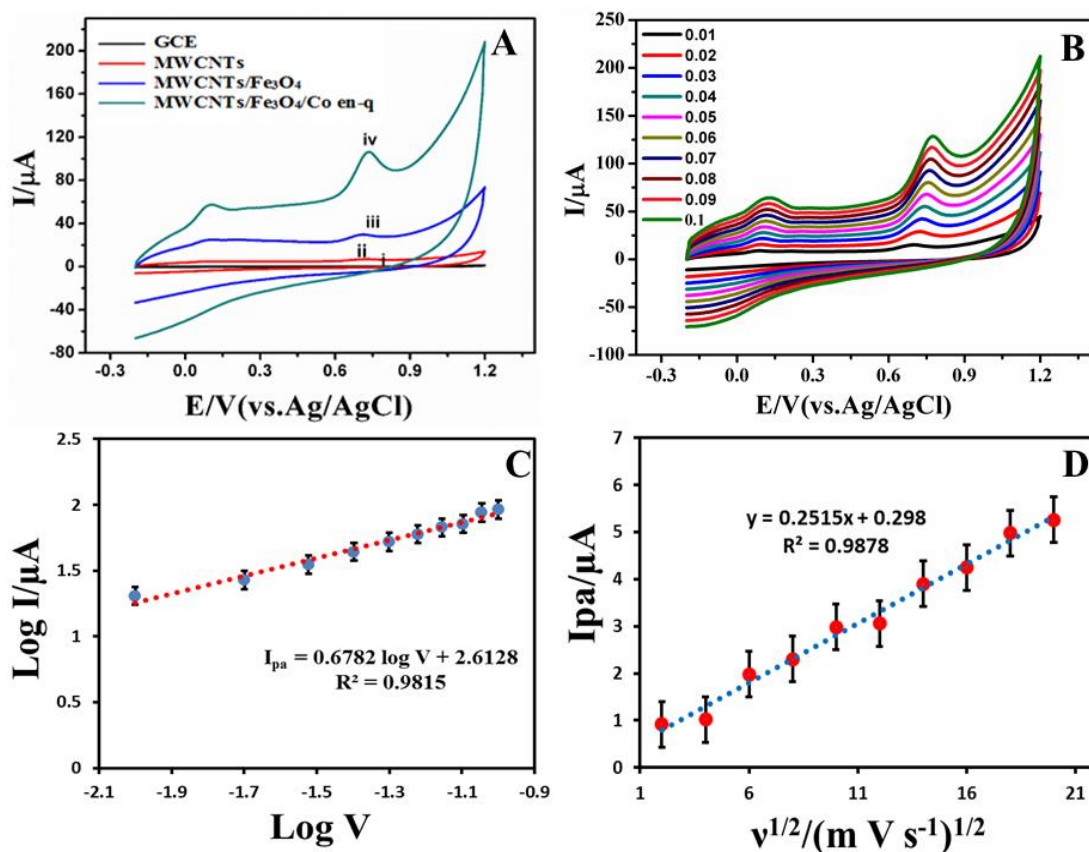
Figure 3. (A) Cyclic voltammograms of 0.1 mM RIF in 0.1M PBS (pH 7.5) **(i)** GCE, **(ii)** MWCNTs, **(iii)** MWCNTs/Fe_3O_4NPs/GCE, **(iv)** Co en-q/MWCNTs/Fe_3O_4NPs/GCE. **(B)** Cyclic voltammograms of 0.1mM RIF at scan rates 0.01, 0.02, 0.03, 0.04, 0.05, 0.06, 0.07, 0.08 0.09, and 0.1V s^{-1}. **(C)** Linear relationship of log (I_{pa}) and log (v) **(D)** The relationship between anodic peak currents (I_{pa}) vs square root of scan rate.

Fig. 3A shows the electrochemical behaviors of RIF on bare GCE (black line), MWCNTs/GCE (red line), Fe_3O_4/MWCNTs/GCE (blue line) and Co en-q/ Fe_3O_4/MWCNTs/GCE (green line), investigated by the cyclic voltammetry.

The cyclic voltammograms of RIF gave two anodic peaks at + 0.1 V and + 0.7 V potentials. The bare GCE showed very low anodic peak currents 28 µA, whereas the MWCNTs/GCE and Fe_3O_4/MWCNTs/GCE showed 75 µA and 150 µA currents respectively (S Fig. 1). The Co en-q/ Fe_3O_4/MWCNTs/GCE showed the higher peak currents (220µA) than the remaining modified electrodes (fig. 3B). It can be concluded that the Co en-q has actively participated in the high electron transfer between the RIF molecule and fabricated electrode. Moreover, a graph drawn between log V and log I_{pa} shows a linear relationship and can be expressed as $I_{pa} = 0.6782 \log V + 2.6128$ ($R^2 = 0.9815$ fig. 3C). Simultaneously a graph was drawn between the anodic peak currents and square root of the scan rate ($v^{1/2}$), and the resulting linear equation can be express as $I_{pa} = 0.2515 v^{1/2} + 0.298$ ($R^2 = 0.9878$) (fig. 3D). The results confirmed that the diffusion controlled mechanism is usual for the overall electrochemical reaction of RIF at the fabricated electrode surface [28-30]. According to these results an improved electrocatalytic effect of RIF at the fabricated electrodes is due to the increased surface to volume ratio and electronic conductivity. The fabricated electrode surface area was calculated by Randles-Sevick equation [31].

$$I_{pa} = 2.69 \times 10^5 \, A \, C_0 \, n^{3/2} D_R \, v^{1/2} \qquad\qquad (2)$$

Where I_{pa} denotes the anodic peak current, A the electrode area (A is surface area electrode, r_e is the radius of the rotating disc electrode, ($A = \pi r_e^2$)), C_o is the concentration of RIF, n is the number of electrons involved in the reaction, D_R is the analyte diffusion coefficient (cm^2/s), v is scan rate (V s^{-1}). From the above equation the fabricated electrode and GCE surface area was estimated to be 10.03 and 3.14 mm^2 respectively. The increased surface area and the presence of adsorptive sites in Co en-q resulting in the significant increase the anodic currents. Due to the high density of active sites and ketonic functional group in Co en-q, accelerating the electron transfer between fabricated electrode and RIF. Based on the obtained results indicates the Co en-q/ Fe_3O_4/MWCNTs/GCE sensor surface area was approximately three times greater than the GCE surface. Which is responsible for the high electrochemical oxidation of RIF (Scheme 1).
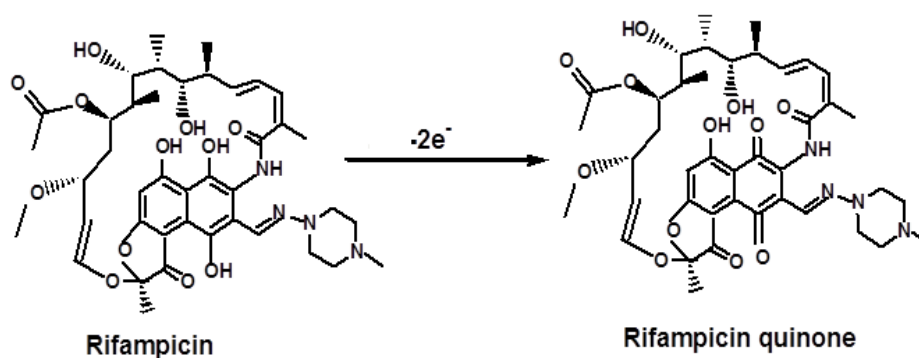
Scheme 1. Schematic illustration of the electro oxidation reaction of RIF leading to rifampicin quinone formation.

3.3. Effect of Co en-q concentration on the sensor response

The CV study was performed in order to determine the optimum concentration of Co en-q within the range of 1.2 to 14 µg mL^{-1}. The anodic peak currents were gradually increasing with the increase in concentrations Co en-q, from 1.2 to 6 µg mL^{-1} (Fig. 4). Beyond the concentration 6 µg mL^{-1} the current response decreased gradually. This is due to the steric hindrance of more accumulation of enzyme on the surface of the electrode, leading to inhibition of the electronic communication between RIF and the fabricated electrode. The concentration of Co en-q was (6 µg mL^{-1}) selected as optimum for the present study.
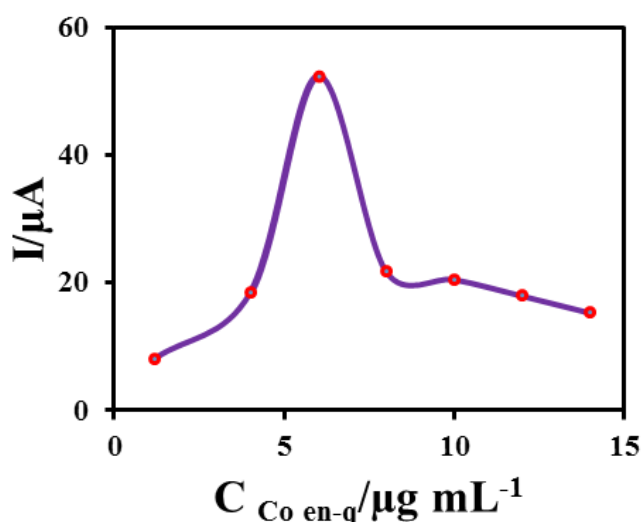
**Figure 4.** Effect of the Co en-q concentration on the response of the Co en-q/ Fe$_3$O$_4$/MWCNTs/GCE in 0.1 mM of RIF with PBS (pH 7.5) at ambient temperature.

3.4. Influence of pH, scan rates and deposition time

The electrochemical oxidation of RIF basically depends upon the range of the supporting electrolyte pH, because it affects of the responses of peak currents and peak potentials. Fig. 5A shows the electrochemical sensing abilities of modified electrode in the pH ranges from 2.5 to 9.5. The RIF gave well-defined anodic peak with high current response at pH 7.5, beyond pH 7.5 the peak current responses gradually decreased. According to these results pH 7.5 was choosen as optimum pH. Additionally, the relationship between peak potentials and pH values were plotted and shown in fig 5B.

The linear regression equation obtained in fig. 5B, E_p (V) = - 0.0688 pH + 0.8579 with correlation coefficient with R^2 = 0.9877 was approximately equal to the previously reported regression equation E_p (V) = -0.0591 pH + 0.3296 with R^2 = 0.9897[32, 33]. Based on the above results it is evident that two electrons were involved in electrode oxidation process. Fig. 3B shows the effect of scan rates ranges from 0.01 to 0.1 mVs^{-1} on the current response of RIF at the fabricated electrode. It can be seen that by increasing the scan rates, the anodic peak currents increase linearly with maximum peak current 0.1 m V s^{-1}. Thus 0.1 m V s^{-1} was used as an optimum scan rate for this study. It was

possible to calculate current efficiency of RIF at electrode deposition process based on the polarization curves (Fig.5C). The effect of deposition time was also monitored from 30 to 150 s at scan rate of 0.1 mV s^{-1} at pH 7.5 resulted in a deposition potential of -0.187 V. The current responses were maximum at 90 s, thus it is preferred as optimum deposition time for the entire study (Fig. 5C).
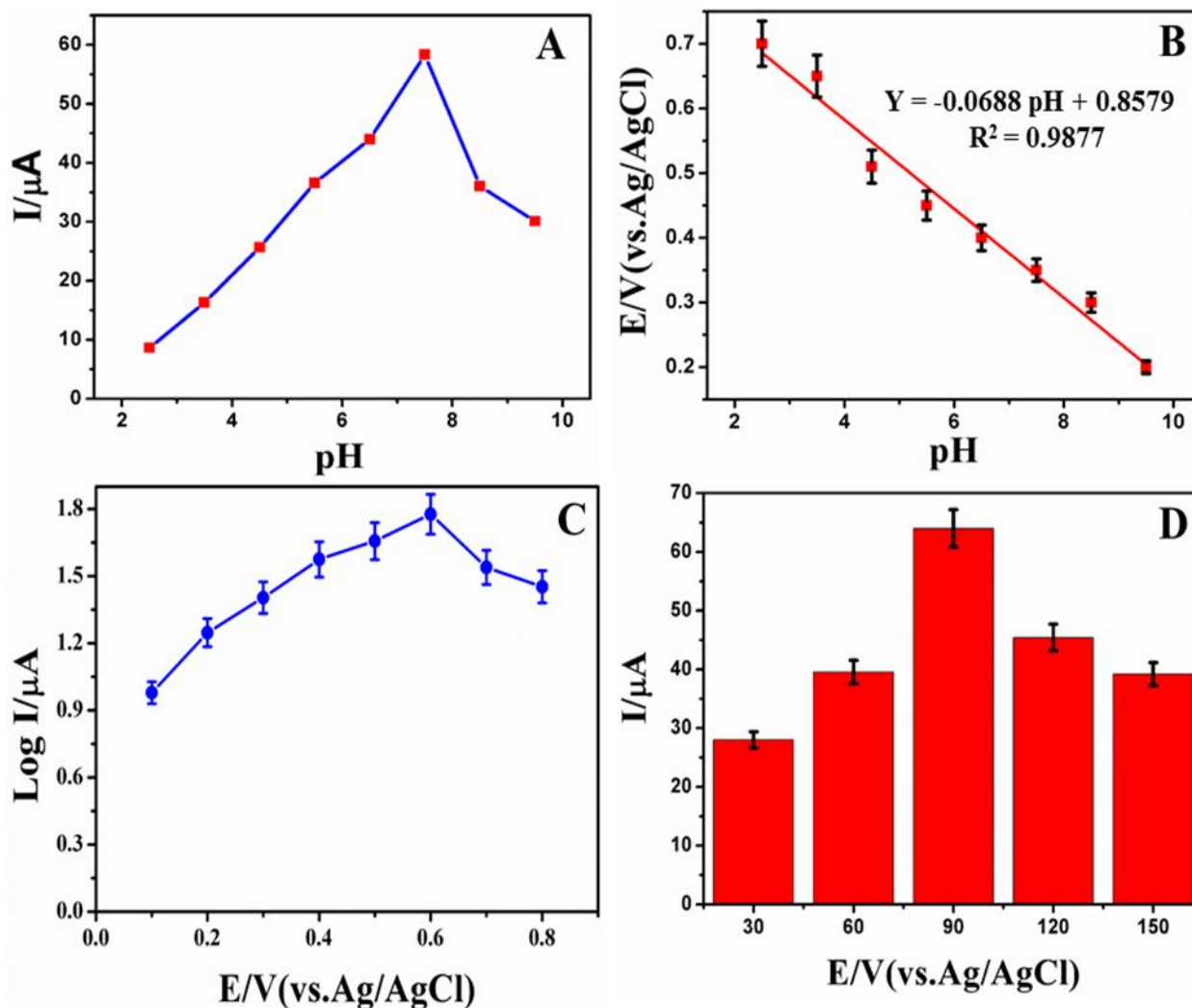
**Figure 5. (A)** Peak potential and peak currents response with pH ranges 2.5, 3.5, 4.5, 5.5, 6.5, 7.5, 8.5, and 9.5. **(B)** Peak potentials and pH **(C)** Polarization curve of Co en-q/ Fe$_3$O$_4$/MWCNTs/GCE. **(D)** Peak current responses vs different deposition time ranges 30, 60, 90, 120 and 150 s.

3.5. Determination of sensitivity of the developed sensor

DPV was used to evaluate the sensitivity of the fabricated sensor towards RIF. The working method parameters (scan rate 0.1 V s^{-1}, deposition time 90 s, pulse amplitude 0.050 mV and pulse time 0.040 s) were employed for the differential pulse voltammetric determination. The peak current responses on the concentration of RIF were obtained in the linear range 2 to 20 μM. The calibration

curves were linear over the concentration ranges from 2 to 20 μM for DPV. The calibration curve was then plotted for the concentration of RIF versus peak currents (Fig. 6).
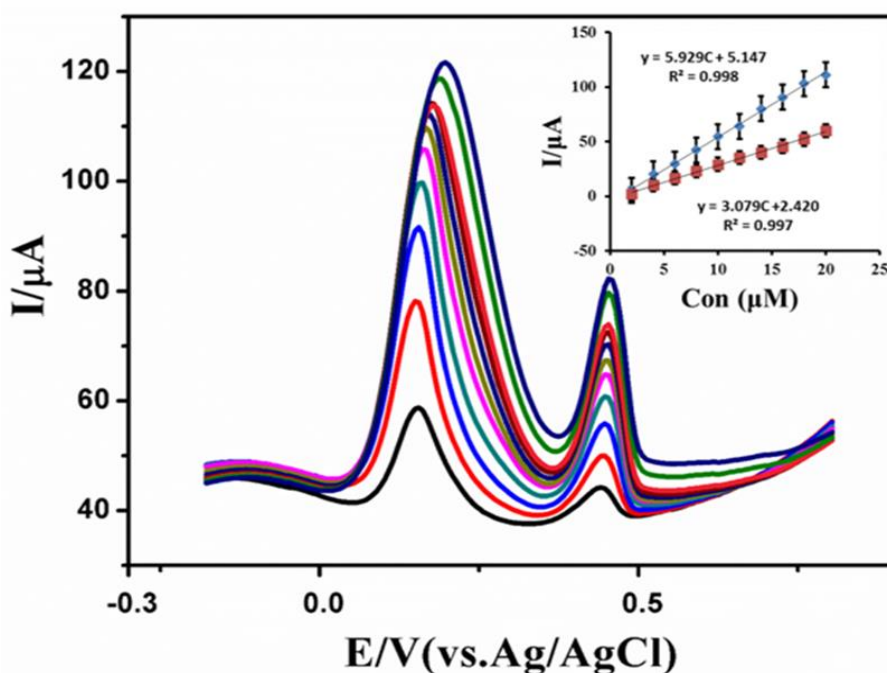
Figure 6. DPV recorded at Co en-q/Fe$_3$O$_4$NPs/MWCNTs/GCE at different concentrations of RIF (2– 20 μM), inset: plot show for linear dependence of I$_{pa}$ versus RIF. (Conditions for DPV pH: 7.5, accumulation time: 90 s, accumulation potential: 0.1Vs^{-1}, pulse amplitude: 0.050 V, pulse time 0.040 s).

Table 1. Comparison of some characteristics of the previously reported modified electrodes with Co en-q/ Fe$_3$O$_4$NPs/MWCNTs/GCE.

Electrode	Technique	LOD/ (μM)	Linear Range/ (μM)	Buffer/ pH	Ref
β-CD/PPY/Pt[1]	CA	1.69	10-50	PBS;7.06	[11]
AgNPs/PANSA/EGCYP2E1[2]	CV;DPV	0.05	2 - 14	PBS;7.4	[12]
CPE[3]	SWAdASV	0.05	0.1-6	PBS;7	[34]
Ni(OH)$_2$–RGO–GCE[4]	LSV	2.34	0.004–10	PBS;7	[13]
Co en-q/ Fe$_3$O$_4$NPs/MWCNTs/GCE[5]	CV; DPV	0.032	2-20	PBS;7	This work

β-CD/PPY/Pt- ß-cyclodextrin-polypyrrole coated on platinum electrode; Au/PVP-AgNPs/PANSA/EG-CYP2E1- Polyvinyl pyrrolidone/silver nanoparticles/poly (8-anilino-1-naphthalene sulphonicacid); CPE-Carbon paste electrode; Ni(OH)$_2$–RGO–GCE- Nickel hydroxide nanoparticles-reduced graphene oxide nanosheets coated on glassy carbon electrode; Coenzyme q/ Fe$_3$O$_4$NPs/MWCNTs/GCE- Coenzyme q- Fe$_3$O$_4$ nanoparticles-multiwall carbon nanotubes coated on GCE; CA-chronoamperometry; CV-Cyclic voltammetry; DPV- Differential pulse polarography; SWAdASV-Square-wave adsorptive anodic stripping voltammetry; LSV-Linear sweep voltammetry; PBS-Phosphate buffer solution.

The linear regression equation can be expressed as $I_{pa} = 5.929 \, C_{RIF}$ (µM) + 5.147 with correlation coefficient [($R^2 = 0.998$) and $I_{pa} = 3.079 \, C_{RIF}$ (µM) + 2.420 with correlation coefficient ($R^2 = 0.997$)] was determined by DPV. The limit of detection (LOD) and limit of quantization (LOQ) was calculated based on signal to noise ratios, by using the following equations.

$$LOD = \frac{3S_B}{b} \qquad\qquad (3)$$

$$LOQ = \frac{10S_B}{b} \qquad\qquad (4)$$

Where S_B is the standard deviation of the blank solution for three different runs, and b is the slope of the calibration curve. The limit of detection and limit of quantification was found to be 0.032 µM, 0.413 µM and 1.069 µM, 1.258 µM for anodic peak I and peak II respectively. The results obtained indicated that the Co en-q/ Fe_3O_4NPs/MWCNTs/GCE was an excellent biosensor for the sensitive determination of RIF. Compared to previous reports sensors comparison table (Table 1).

3.6. Interference study

Table 2. Effects of interferents on the anodic peak current responses for 0.1mM RIF at Co en-q/ Fe_3O_4NPs/MWCNTs/GCE based electrochemical sensor.

Interference species	Interferents/molar ratio of RIF	Responses ratio (%)
SO_4^{-2}	200	< 1.05
	400	< 2.09
Br^-	200	< 0.9
	400	< 1.06
NO_3^-	200	< 1.35
	400	< 2.49
Ni^{2+}	200	< 0.85
	400	< 1.79
Fe^{3+}	200	< 1.02
	400	< 2.89
K^+	200	< 0.95
	400	< 2.01
Glutamic acid	200	< 1.05
	400	< 2.09
Uric acid	200	< 1.25
	400	< 2.49
Folic acid	200	< 1.09
	400	< 3.01

The interference effect of the Co en-q/ Fe_3O_4NPs/MWCNTs/GCE with 0.1 mM RIF was evaluated in the presence of some organic, inorganic, and some other foreign interfering molecules through DPV method. The inorganic interference ions like $SO4^{-2}$, Br^-, NO_3^-, Ni^{2+}, Fe^{3+} and K^+ do not interfere with electrochemical response of RIF. The real samples were also investigated with the possible interference of these pharmaceutical samples with RIF peaks (The real pharmaceutical sample preparations and brands are mentioned in section 2.5). In addition, the organic interference like

glutamic acid, uric acid and folic acid do not interfere with the current response (≤6%) when present in 0.1 mM concentration of RIF. Based on the current results, the fabricated electrode was successfully used for the quantification of RIF in PBS (pH 7.5) and the results of this study are summarized in Table 2.

3.7. Analytical performances of the modified sensor

The repeatability of the fabricated sensor performance was calculated by using the anodic currents generated by the various analyte concentrations taken 10 times in a day. In the following day responses of 10 different preparations of electrodes in 0.1 M RIF solution were again tested. It was found that the repeatability decreased less than 5% to original current responses. In order to investigate the stability of Co en-q/ Fe_3O_4NPs/MWCNTs/GCE was measured by the CV peak currents in PBS with 0.1 M RIF was tested after 50 days. The current responses of the final biosensor remained at 80.25% of the initial response after 40 days as indicated in S Fig. 2A.

4. CONCLUSION

The present study demonstrated a simple and facile method for the modification of GCE with MWCNTs/Fe_3O_4NPs and Co en-q for the determination of RIF. The resulting MWCNTs, MWCNTs/Fe_3O_4NPs have been successfully characterized by using FT-IR, XRD and TEM. The electrochemical behaviour of RIF on the bare GCE and modified Co en-q/ Fe_3O_4/MWCNTs/GCE were observed using cyclic voltammetry. The obtained cyclic voltammetry results indicate the outstanding electrochemical sensing performance of the biosensor, with an increase (approximately eight-folds) of anodic peak currents. This indicates the high electrochemical response ability of developed biosensor towards the oxidation of RIF compared to the previous electrodes. Under the optimal experimental conditions, the anodic peak currents of RIF increased linearly within the concentration range 2-20 μM bearing the correlation coefficients of $R^2 = 0.998$, and $R^2 = 0.997$ respectively. The LOD and LOQs were calculated and found to be 0.032 μM, 0.413 μM and 1.069 μM, 1.258 μM for peak I and peak II respectively. This also reveals the high sensitivity and selectivity of the fabricated biosensor without interferents. The biosensor exhibited good reproducibility and stability as well as the successful analytical applications. The proposed biosensor was certainly adequate for the determination of RIF in the commercial pharmaceutical sample.

SUPPLEMENTARY INFORMATION
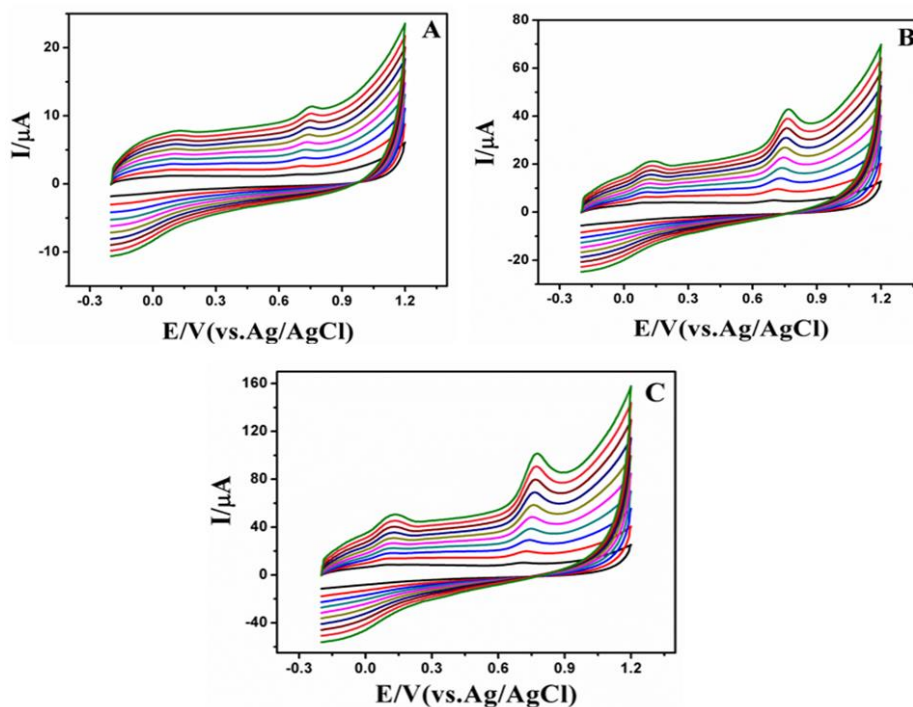
S Figure 1. Cyclic Voltammograms of RIF with **(A)** Bare GCE, **(B)** MWCNTs/GCE, (C) Fe$_3$O$_4$NPs/MWCNTs/GCE at various scan rates ranges 0.01, 0.02, 0.03, 0.04, 0.05, 0.06, 0.07, 0.08, 0.09 and 0.1V s-1.
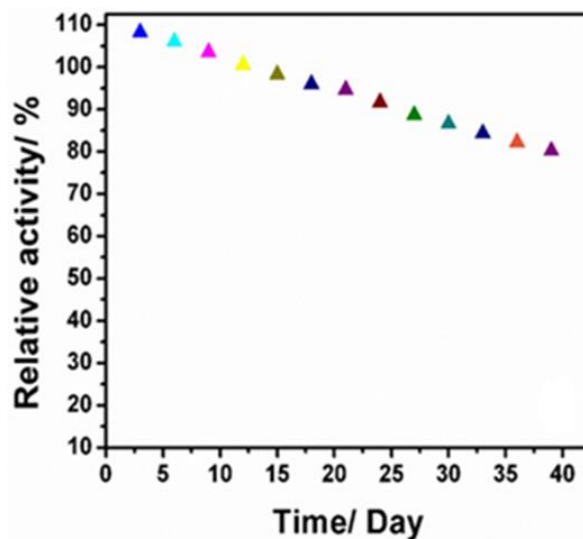
S Figure 2. (A) Stability for Co en-q/Fe$_3$O$_4$NPs/MWCNTs/GCE

References

1. W. Chen, B. Unnikrishnan, S.M. Chen, *Int. J. Electrochem. Sci.,* 7 (2012) 9138.
2. S. Cheemalapati, S. Palanisamy, S.M. Chen, *Int. J. Electrochem. Sci.,* 8 (2013) 3953.
3. M.S.M. Quintino, L. Angnes, *J. Pharm. Biomed. Anal.* 42 (2006) 400.

4. N.F. Atta, A. Galal, F.M. Abu-Attia, S.M. Azab, *Electrochim. Acta* 56 (2011) 2510.
5. A.K. Hemanth Kumar, I. Chandra, R. Geetha, K.S. Chelvi, V. Lalitha, G. Prema, *Indian J Pharmacol*, 36 (2004) 231.
6. J.B. Lecaillon, N. Febvre, J.P. Metayer, C. Souppart, *J. Chromatogr. B:Anal. Technol. Biomed. Life Sci.* 145 (1978) 319.
7. K. Asadpour-Zeynali, P. Soheili-Azad, *Electrochim. Acta* 55 (2010) 6570.
8. M. A. Karimi, A. H. Mehrjardi, M. M. Ardakani, R. B. Ardakani, M. H. Mashhadizadeh, S. Sargazi, *Int. J. Electrochem. Sci.,* 5 (2010) 1634.
9. J. van den Boogaard, G.S. Kibiki, E.R. Kisanga, M.J. Boeree, R.E. Aarnoutse, *Antimicrob. Agents Chemother.* 53 (2009) 849.
10. S.T. Girousi, I. Gherghi, M.K. Karava, *J. Pharm. Biomed. Anal.* 36 (2004) 851.
11. M.A. Alonso Lomillo, O. Domínguez Renedo, M.J. Arcos Martínez, *Electrochim. Acta* 50 (2005) 1807.
12. R.F. Ajayi, U. Sidwaba, U. Feleni, S.F. Douman, O. Tovide, S. Botha, *Electrochim. Acta* 128 (2014) 149.
13. M.A. Alonso Lomillo, J.M. Kauffmann, M.J. Arcos Martinez, *Biosens. Bioelectron.* 18 (2003) 1165.
14. R.A. Couto, M.B. Quinaz, *Sensors*, 16 (2016) 1015.
15. M. Ma, Z. Miao, DI. Zhang, X. Du, Y. Zhang, C. Zhang, J. Lin, Q. Chen, *Biosens. Bioelectron.* 64 (2015) 477.
16. K.S. Loh, Y.H. Lee, A. Musa, A.A. Salmah, I. Zamri, *Sensors* 8 (2008) 5775.
17. X. Cao, N. Wang, *Analyst,* 136 (2011) 4241.
18. R.A. Couto, M.B. Quinaz, *Sensors,* 16 (2016) 1015.
19. L. Ernster, G. Dallner, *Biochim. Biophys. Acta, Mol. Basis Dis.* 1271 (1995) 195.
20. S.A. Kahani, Z. Yagini, *Bioinorg. Chem. Appl.* 2014 (2014) 384984.
21. S. Ahmad, U. Riaz, A. Kaushik, J. Alam, *J. Inorg. Organomet. Polym.* 19 (2009) 355.
22. S. Asgari, Z. Fakharib, S. Berijanic, *JNS,* 4 (2014) 55.
23. L. Yan, S. Li, H. Yu, R. Shan, B. Du, T. Liu, *Powder Technology* 301 (2016) 632.
24. V.A.J. Silva, P.L. Andrade, M.P.C. Silva, A. Bustamante D, L. De Los Santos Valladares, J. Albino Aguiar, *J. Magn. Magn. Mater.* 343 (2013) 138.
25. S.A. Kulkarni, P. S. Sawadh, K. K. Kokate, International Conference on Benchmarks in Engineering Science and Technology ICBEST, *Proceedings published by Int. J. Computer Applications (IJCA)*, (2012) 17.
26. N. Arsalani, *eXPRESS Polymer Letters,* 4 (2010) 329.
27. W.H. Zhou, C.H. Lu, X.C. Guo, F.R. Chen, H. H. Yang, X.R. Wang, *Supplementary Material (ESI) for J. Mater. Chem.* 2010.
28. R.S. Nicholson, I. Shain, *Anal. Chem.* 36 (1964) 706.
29. I. Streeter, G.G. Wildgoose, L. Shao, R.G. Compton, *Sens. Actuators B* 133 (2008) 462.
30. L. Xiao, L. Wi, G.G. Wildgoose, R.G. Compton, *Sens. Actuators B* 138 (2009) 524.
31. N.K. Bhajanthri, V.K. Arumugam, R. Chokkareddy, G.G. Redhi, *J. Mol. Liq.* 222 (2016) 370.
32. S. Rastgara, S. Shahrokhiana, *Talanta* 119 (2014) 156.
33. K. Asadpour-Zeynali, F. Mollarasouli, *Biosens. Bioelectron.* 92 (2017) 509.
34. M. Pumera, *Chem Rec,* 9 (2009) 211.